Structure of spherical three-dimensional Coulomb crystals

P. Ludwig,[1,2] S. Kosse,[1,3] and M. Bonitz[1]

[1]*Institut für Theoretische Physik und Astrophysik, Christian-Albrechts-Universität zu Kiel, Leibnizstrasse 15, 24098 Kiel, Germany*
[2]*Fachbereich Physik, Universität Rostock, l8051 Rostock, Germany*
[3]*Sektion Physik, Ernst-Moritz-Arndt Universität Greifswald, Domstrasse 10a, l7487 Greifswald, Germany*

An analysis of the structural properties of three-dimensional Coulomb clusters confined in a spherical parabolic trap is presented. Based on extensive high-accuracy computer simulations the shell configurations and energies for particle numbers in the range $60 \leq N \leq 160$ are reported. Further, the intrashell symmetry and the lowest metastable configurations are analyzed for small clusters and a different type of excited state that does not involve a change of shell configuration is identified.

Spatially confined charged particle systems have a number of unique properties not observed in conventional *quasineutral macroscopic* plasmas of electrons and ions in discharges or solids, electrons and holes in highly excited semiconductors, and so on. With the help of confinement potentials it has now become routine to trap, for long periods of time, *plasmas of a single charge* (nonneutral plasmas), e.g., electrons and ions and even positrons in Paul and Penning traps [1–3] (for an overview see [4]), or colloidal (dusty) plasmas in discharge chambers (e.g., [5]). By varying the confinement strength researchers have achieved liquid behavior and even Coulomb crystallization of ions [3,6] and dust particles [7,8]. These strong correlation phenomena are of exceptional current interest in a large variety of fields ranging from astrophysics (interior of giant planets) and high-power laser compressed laboratory plasmas, to condensed matter and quantum dots [9], etc. Coulomb (Wigner) crystals are expected to exist in many white dwarf stars.

A particular property of trapped small ($N \lesssim 1000$) clusters in spherical traps is the occurrence of concentric shells with characteristic occupation numbers, shell closures, and unusual stable "magic" configurations. Due to their close similarity to nuclei, metal clusters, or atoms, these systems are sometimes called "artificial atoms." A significant number of papers has been devoted to the exploration of the energetically lowest shell configuration (ground state) and metastable ("excited") states of two-dimensional (2D) artificial atoms (e.g., [10–12] and references therein).

On the other hand, *three-dimensional spherical Coulomb crystals* (3D SCCs) have been observed in laboratory experiments with ultracold ion plasmas [3,6], and the interest in them is now rapidly growing [13] after their prediction in expanding laser-cooled neutral plasmas [14] and their experimental creation in dusty plasmas as well [15]. This raises a question about theoretical results for the configurations of spherical 3D Coulomb crystals, which is the subject of this paper. These results are expected to be an important reference for the above experiments but also for other possible candidates for 3D crystals, including semiconductor nanostructures. It is natural to start with an analysis of the ground state and lowest metastable states, deferring finite temperature and melting properties [e.g., [16]] and also deviations

from an isotropic Coulomb interaction to a subsequent study.

The theoretical analysis of 3D SCCs is much more involved than in 2D and has so far mostly been restricted to small cluster sizes with often conflicting results (e.g., [17–19] and references therein). Rafac *et al.* [18], correcting earlier results, identified the first shell closure at $N=12$ (the 13th particle is the first to occupy a second shell) and presented detailed data, including ground state energies for $N \leq 27$, but they missed the onset of the third shell, as did Hasse and Avilov [17]. Tsuruta and Ichimaru extended the table to $N=59$ [19]. The most extensive data, for up to a few thousand particles, have been presented by Hasse and Avilov [17] and has been a valuable reference for theoretical and experimental groups. However, as our calculations show, their tables contain excited states rather than the true ground states for $N=28$–31, 44, 54 and practically for all $N > 63$ (except for $N=66$). Therefore, it is an important task to obtain the correct ground state shell configurations and cluster properties for particle numbers beyond $N=60$.

The reason for the computational difficulties is the existence of a large number of excited (metastable) states which are energetically close to the ground state; with increasing N this number grows exponentially whereas the energy difference rapidly vanishes. Calculations with a too low accuracy will then frequently miss the correct ground state. Therefore, we use an improved computational strategy which drastically reduces the probability of such misses (see below).

Model: we consider N classical particles with equal charge q and mass m interacting via the Coulomb force and being confined in a 3D isotropic harmonic trap with frequency ω with the Hamiltonian

$$H_N = \sum_{i=1}^{N} \frac{m}{2}\dot{r}_i^2 + \sum_{i=1}^{N} \frac{m}{2}\omega^2 r_i^2 + \sum_{i>j}^{N} \frac{q^2}{4\pi\varepsilon|\mathbf{r}_i - \mathbf{r}_j|}. \quad (1)$$

Despite its simplicity, the model (1) captures the basic properties of a multitude of classical systems and serves as an important reference point also for more complex 3D systems. Below we will use dimensionless lengths and energies by introducing the units $r_0 = (q^2/2\pi\varepsilon m\omega^2)^{1/3}$ and $E_0 = (m\omega^2 q^4/32\pi^2\varepsilon^2)^{1/3}$, respectively.

TABLE I. Shell configurations, energy per particle for the lowest-lying states (for the excited states the energy difference with respect to the ground state is given in italics), mean radius of the outer shell r_1, symmetry parameter G_M, Eq. (2), and number of Voronoi M-polygons $N(M)$ in brackets. For $N=4$, $N(3)=4$, and for $N=5$, $N(3)=2$, $N(4)=3$.

N	Configuration	E/N	r_1	G_4 [$N(4)$]	G_5 [$N(5)$]	G_6 [$N(6)$]
2	(2)	0.750000	0.5000	–	–	–
3	(3)	1.310371	0.6609	–	–	–
4	(4)	1.785826	0.7715	–	–	–
5	(5)	2.245187	0.8651	1.000 [3]	–	–
6	(6)	2.654039	0.9406	1.000 [6]	–	–
7	(7)	3.064186	1.0106	1.000 [5]	1.000 [2]	–
8	(8)	3.443409	1.0714	0.641 [4]	0.821 [4]	–
9	(9)	3.809782	1.1269	0.965 [3]	0.957 [6]	–
10	(10)	4.164990	1.1783	1.000 [2]	0.861 [8]	–
	(9,1)	*0.021989*	1.2453	0.965 [3]	0.957 [6]	
11	(11)	4.513275	1.2265	0.940 [2]	0.894 [8]	1.000 [1]
	(10,1)	*0.009876*	1.2878	1.000 [2]	0.861 [8]	–
12	(12)	4.838966	1.2700	–	1.000 [12]	–
	(11,1)	*0.015345*	1.3286	0.938 [2]	0.895 [8]	1.000 [1]
13	(12,1)	5.166798	1.3659	–	1.000 [12]	–
	(13)	*0.005061*	1.3130	1.000 [1]	0.894 [10]	0.932 [2]
14	(13,1)	5.485915	1.4033	–	0.893 [10]	0.933 [2]
	(14)	*0.003501*	1.3527	1.000 [1]	0.938 [12]	1.000 [2]
15	(14,1)	5.792094	1.4383	–	0.938 [12]	1.000 [2]
	(15)	*0.009031*	1.3906	–	0.885 [12]	0.963 [3]
16	(15,1)	6.093421	1.4719	–	0.882 [12]	0.962 [3]
	(16)	*0.012200*	1.4266	–	0.897 [12]	0.993 [4]
	(16)	*0.012635*	1.4267	–	0.747 [12]	0.884 [4]
17	(16,1)	6.388610	1.5042	–	0.891 [12]	0.993 [4]
	(16,1)	*0.000365*	1.5042	–	0.746 [12]	0.884 [4]
	(17)	*0.015766*	1.4611	–	0.738 [12]	0.810 [5]
18	(17,1)	6.678830	1.5353	–	0.738 [12]	0.810 [5]
	(18)	*0.018611*	1.4941	1.000 [2]	0.829 [8]	0.920 [8]
19	(18,1)	6.964146	1.5654	1.000 [2]	0.827 [8]	0.920 [8]
20	(19,1)	7.247181	1.5946	–	0.838 [12]	0.918 [7]
	(18,2)	*0.004264*	1.6285	0.991 [2]	0.824 [8]	0.913 [8]
21	(20,1)	7.522378	1.6226	–	0.792 [12]	0.917 [8]
	(19,2)	*0.004668*	1.6557	–	0.847 [12]	0.927 [7]
22	(21,1)	7.795469	1.6499	1.000 [1]	0.877 [10]	0.880 [10]
	(21,1)	$2.5 \cdot 10^{-7}$	1.6499	1.000 [1]	0.859 [10]	0.866 [10]
	(20,2)	*0.000976*	1.6821	–	0.801 [12]	0.935 [8]
	(20,2)	*0.001053*	1.6820	–	0.763 [12]	0.909 [8]

To find the ground and metastable states, we used classical molecular dynamics (MD) together with an optimized version of the standard simulated annealing method. Starting with a random initial configuration of N particles, the system is cooled continuously until all momenta are zero and the particles settle in minima of the potential energy surface. Depending on the particle number, the cooling down process was repeated between several hundred and several thousand times until every one of the computed low-energy states was found more than a given number of times (typically 10–100) assuring a high probability that the ground state has been found. Crucial for a high search efficiency is the use of an optimized MD time step (it has to be chosen not too small to avoid trapping in local potential minima). The results are shown in Tables I and II.

Consider first the ground state shell configurations beyond the previously reported results [18,19] (see Table II). Closure of the second shell is observed twice: for $N=57$ [19] and 60. Further, we have found the closure of the third shell to occur at $N=154$; all larger clusters have at least four shells (in the ground state). The "noble-gas-like" closed shell clusters are particularly stable, but a few others also have a comparatively high binding energy (addition energy change) $\Delta_2(N) = E(N+1) + E(N-1) - 2E(N)$. Tsuruta and Ichimaru [19]

TABLE II. Ground state shell configurations, energy per particle for the lowest-lying states, and mean shell radii $r_{1,2,3}$ [20].

N	Configuration	E/N	r_1	r_2	r_3
28	(25,3)	9.348368	1.8525	0.6889	–
29	(25,4)	9.595435	1.8992	0.7987	–
30	(26,4)	9.838965	1.9198	0.7961	–
31	(27,4)	10.079511	1.9399	0.7926	–
44	(36,8)	13.020078	2.2454	1.0845	–
54	(44,10)	15.085703	2.4186	1.1872	–
55	(43,12)	15.284703	2.4618	1.2772	–
56	(44,12)	15.482144	2.4743	1.2770	–
57	(45,12)	15.679350	2.4869	1.2763	–
58	(45,12,1)	15.875406	2.5126	1.3765	–
59	(46,12,1)	16.070103	2.5247	1.3764	–
60	(48,12)	16.263707	2.5236	1.2754	–
64	(49,14,1)	17.027289	2.6101	1.4478	–
65	(50,14,1)	17.215361	2.6212	1.4477	–
80	(60,19,1)	19.936690	2.8369	1.6002	–
84	(61,21,2)	20.632759	2.9064	1.7140	0.5426
94	(67,24,3)	22.325841	3.0347	1.8356	0.7001
95	(67,24,4)	22.491878	3.0522	1.8848	0.8089
96	(68,24,4)	22.657271	3.0606	1.8846	0.8083
97	(69,24,4)	22.822032	3.0687	1.8849	0.8095
98	(69,25,4)	22.986199	3.0864	1.9055	0.8081
99	(70,25,4)	23.149758	3.0945	1.9056	0.8071
100	(70,26,4)	23.312759	3.1117	1.9259	0.8055
101	(70,27,4)	23.475164	3.1291	1.9450	0.8028
103	(72,27,4)	23.798274	3.1451	1.9443	0.8017
105	(73,28,4)	24.120223	3.1696	1.9641	0.8020
107	(75,28,4)	24.439666	3.1850	1.9640	0.8011
109	(77,28,4)	24.757151	3.2005	1.9638	0.8006
111	(77,29,5)	25.072584	3.2322	2.0249	0.8968
113	(77,30,6)	25.385842	3.2637	2.0831	0.9640
115	(77,32,6)	25.697308	3.2949	2.1162	0.9630
117	(79,32,6)	26.007089	3.3094	2.1158	0.9622
119	(81,32,6)	26.315442	3.3237	2.1156	0.9624
121	(83,32,6)	26.622118	3.3379	2.1154	0.9614
123	(83,34,6)	26.927195	3.3672	2.1493	0.9625
125	(84,34,7)	27.230458	3.3884	2.1850	1.0340
128	(85,35,8)	27.682123	3.4235	2.2358	1.0922
130	(86,36,8)	27.981234	3.4445	2.2501	1.0917
133	(88,37,8)	28.427062	3.4718	2.2642	1.0912
135	(88,38,9)	28.722421	3.4992	2.3110	1.1436
137	(90,38,9)	29.016328	3.5119	2.3110	1.1440
139	(91,39,9)	29.308774	3.5316	2.3251	1.1430
141	(92,40,9)	29.599900	3.5514	2.3387	1.1417
143	(93,40,10)	29.889733	3.5707	2.3689	1.1932
145	(94,41,10)	30.178106	3.5898	2.3825	1.1920
147	(95,42,10)	30.465219	3.6087	2.3957	1.1923
149	(96,43,10)	30.750998	3.6273	2.4090	1.1926
151	(96,43,12)	31.035390	3.6524	2.4659	1.2814

TABLE II. (*Continued.*)

N	Configuration	E/N	r_1	r_2	r_3
153	(97,44,12)	31.318528	3.6708	2.4781	1.2811
154	(98,44,12)	31.459632	3.6768	2.4777	1.2810
155	(98,44,12,1)	31.600488	3.6887	2.5042	1.3846
156	(98,45,12,1)	31.741100	3.7006	2.5169	1.3839
158	(100,45,12,1)	32.021294	3.7122	2.5166	1.3834
160	(102,45,12,1)	32.300405	3.7238	2.5161	1.3833

found the stable clusters $N=4,6,10,12,19,32,38,56$. For larger clusters the binding energy decreases, and the relative differences rapidly decrease. We found the next particularly stable ones to be $N=81,94,103,116$. The results are shown in Fig. 1. The relative stability of these clusters is linked to a particularly symmetric particle arrangement within the shells which will be analyzed below.

The existence of the shell structure is a marked difference from macroscopic Coulomb systems ($N\to\infty$) and is, of course, caused by the spherical confinement potential. With increasing N the structure of a macroscopic system emerges gradually (see also Ref. [16]). This can be seen from the relative widths $\bar{\sigma}_m \equiv \sigma_m / r_m$ of the mth shell (σ_m denotes the variance of the shell radius r_m). For example, for $N=149$ (starting from the outermost shell) $\bar{\sigma}_1=0.0089$, $\bar{\sigma}_2=0.035$, and $\bar{\sigma}_3=0.032$, whereas for $N=160$ we obtain $\bar{\sigma}_1=0.0091$, $\bar{\sigma}_2=0.033$, and $\bar{\sigma}_3=0.0038$. In both cases the outermost shell is significantly narrower than the second one and this trend becomes more pronounced as N increases. This is easy to understand because the effect of the confinement is strongest at the cluster boundary, i.e., in the outer shell, whereas the inner shells are partially shielded from the trap potential by the surrounding particle shells. In contrast, the behavior of the inner shells is not that systematic: in one case ($N=149$) the third shell is of similar (relative) width as the second; in the other case ($N=160$) the inner shell is much narrower. The reason is symmetry effects which particularly strongly influence the width of the innermost shell (the cluster $N=160$ has a closed inner shell with 12 particles which is very narrow).

In Table I we also provide the first excited states, which correspond to metastable shell configurations that are different from the ground state. While the overall trend is a rapid decrease of the excitation energy (energy gap to the ground state) with increasing N, some additional systematics is observed. Clusters that open a new shell typically possess a close metastable state. For example, for $N=13$ the relative stability of the configurations $\{N,0\}$ and $\{N-1,1\}$ changes, the latter becomes the ground state and the former the first excited state (see Table I). A similar trend is observed not only when a new shell is opened but also when an additional particle moves onto the inner shell between the states $\{N_1-1,N_2\}$ and $\{N_1,N_2-1\}$. Away from these transition points the energy difference increases and eventually another configuration becomes the first excited state.

An interesting observation is that frequently simulations yielding the same shell configuration resulted in different total energies; see, e.g., $N=16,17,22$ in Table I. The differ-
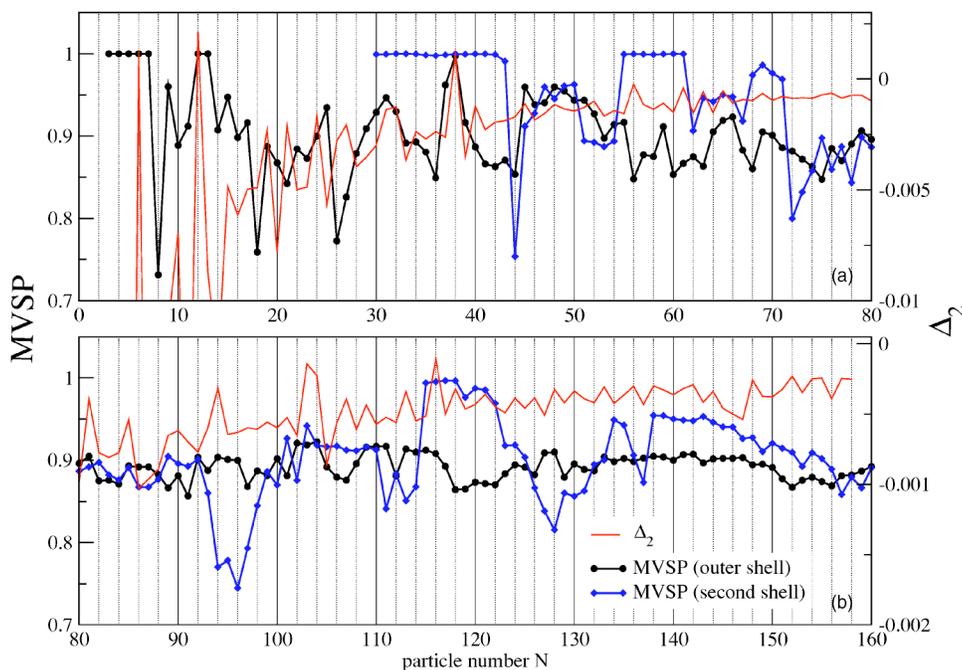
FIG. 1. (Color online) Binding energy Δ_2 (right axis) and mean Voronoi symmetry parameter (MVSP, left axis) for the two outermost cluster shells. (a) $N \leqslant 80$; (b) $80 \leqslant N \leqslant 160$.

ences are much larger than the simulation error; moreover, the energies are reproducible. The obvious explanation is that the state of a cluster is not completely determined by its shell configuration (as is the case in 2D). In addition, there exist further excited states, i.e., a "fine structure," which are due to a *different particle arrangement and symmetry within one shell*. To understand the differences in the structure of these states with the same shell configuration we analyzed the intrashell symmetry by performing a Voronoi analysis, i.e., by constructing polygons around a given particle formed by the lines equally bisecting nearest-neighbor pairs on the shell (see the example of $N=17$ shown in Fig. 2). Interestingly, the two states do not differ with respect to the number of polygons of each kind on the outer shell: there are $N(5)=12$ pentagons and $N(6)=4$ hexagons. However, what is different is the *arrangement of the polygons*: in one case, the four hexagons form a perfect tetrahedron $ABCD$ and are separated from each other by pentagons [see Fig. 2(a)]; in the other two pairs of hexagons touch [see Fig. 2(b)], and the
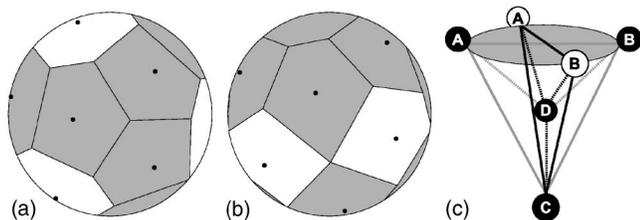

FIG. 2. Voronoi construction for the cluster $N=17$ for the two energetically lowest states with shell configuration $N=\{1,16\}$. White (gray) areas are hexagons (pentagons), indicating the number of nearest neighbors of the corresponding particle (black dot). (a) ground state; (b) first excited ("fine structure") state; (c) arrangement of the four particles surrounded by hexagons; the two states differ by rotation of the edge AB, black (white) circles correspond to case (a) [(b)].

tetrahedron is distorted, as shown in Fig. 2(c). Two edges remain practically constant ($\overline{AB} \approx \overline{CD} \approx 1.63$), but the edge AB rotates with respect to the first case by an angle of 34° resulting in a reduction of edges $\overline{BC}$ and $\overline{AD}$ to about 1.24 while $\overline{AC}$ and $\overline{BD}$ increase to 1.94. From this we conclude that of two states the one with the more symmetric arrangement of the Voronoi polygons, i.e., Fig. 2(a), has the lower energy. To quantify this topological criterion, we introduce the *Voronoi symmetry parameter*

$$G_M = \frac{1}{N_M} \sum_{j=1}^{N_M} \frac{1}{M} \left| \sum_{k=1}^{M} e^{iM\theta_{jk}} \right|, \qquad (2)$$

where N_M denotes the number of all particles j in the shell, each of which is surrounded by a Voronoi polygon of order M (M nearest neighbors), and θ_{jk} is the angle between the jth particle and its kth nearest neighbor. A value $G_5 = 1$ ($G_6 = 1$) means that all pentagons (hexagons) are perfect; the magnitude of the reduction of G_M below 1 measures their distortion. Inspection of the values of G_M for the two {16,1} configurations for $N=17$ (Table I) reveals that the state with lower energy has higher values for both G_5 and G_6 than the second, confirming our observation above. This result is verified for all other N (of course it applies only to states with the same shell configuration).

Having obtained with G_M a suitable symmetry measure that is sensitive to the relative stability of ground and metastable states, we now return to the issue of the overall cluster stability. To this end we compute the *mean Voronoi symmetry parameter* by averaging over all G_M of a given shell weighted with the respective particle numbers $N(M)$. The results for the two outer shells for $N \leqslant 160$ are included in Fig. 1. We clearly see that *magic clusters* have not only a high binding energy but also a prominent symmetry [19]; see in particular $N=12$, 38, 103, and 116.

In summary, in this paper we have presented extensive

simulation results for spherical Coulomb clusters with $N \leq 160$. The observed cluster ground state configurations for $N \geq 60$ differ, in most cases, from the ones previously reported [17] which have a significantly higher energy and thus correspond to excited states of the clusters. The presented tables (for the complete tables, see [20]) should be a valuable reference for experiments with classical 3D Coulomb crystals in dusty plasmas [15], ultracold ions [6], or laser-cooled expanding neutral plasmas [14]. Of course, real experiments with ions or dust grains are likely to exhibit deviations from the simple model (1)—the interaction may deviate from the Coulomb law (e.g., due to screening) and may be direction dependent, the confinement potential is often not perfectly isotropic or parabolic, etc. Therefore, differences in the experimentally observed cluster configurations compared to the above theoretical results may be valuable additional information on imperfections of the experimental setup (possible anisotropic confinement) or on the plasma properties (screening length).

Moreover, the obtained ground state results (shell configurations) are expected to be important also for quantum 3D Coulomb clusters which may exist, e.g., in semiconductor quantum dots in the strong coupling limit. It was found before for 2D systems that, in most cases, the ground state shell configurations in quantum crystals are exactly the same as in the corresponding (essentially simpler) classical crystals [9,12,21]. This remains an interesting question for future analysis.

Further, we have presented an analysis of the lowest excited states of small clusters. Besides metastable states with a shell structure different from the ground state we identified "fine structure" states which are characterized by different particle arrangement within the shells, an important property not existing in 2D crystals. These states have a lower symmetry which is linked to higher values of the total energy.

Finally, knowledge of the lowest metastable states is very important for understanding all dynamic properties of 3D crystals. The metastable states are expected to be of relevance for the collective excitations of the clusters (normal modes that are excited in the system if kinetic energy is supplied) as well as for the melting behavior of the 3D crystals.

[1] F. Diedrich, E. Peik, J. M. Chen, W. Quinnt, and H. Walter, Phys. Rev. Lett. **59**, 2931 (1987).

[2] D. J. Wineland, J. C. Bergquist, W. M. Itano, J. J. Bollinger, and C. H. Manney, Phys. Rev. Lett. **59**, 2935 (1987).

[3] S. L. Gilbert, J. J. Bollinger, and D. J. Wineland, Phys. Rev. Lett. **60**, 2022 (1988).

[4] D. H. E. Dubin and T. M. O'Neill, Rev. Mod. Phys. **71**, 87 (1999).

[5] *Focus on Complex (Dusty) Plasmas*, edited by G. E. Morfill and H. Kersten, special issue of New J. Phys. **5** (2003).

[6] W. M. Itano, J. J. Bollinger, J. N. Tan, B. Jelenkovic, and D. J. Wineland, Science **297**, 686 (1998).

[7] H. Thomas, G. E. Morfill, V. Demmel, J. Goree, B. Feuerbacher, and D. Möhlmann, Phys. Rev. Lett. **73**, 652 (1994).

[8] Y. Hayashi and K. Tachibana, Jpn. J. Appl. Phys., Part 2 **33**, L804 (1994).

[9] A. V. Filinov, M. Bonitz, and Yu. E. Lozovik, Phys. Rev. Lett. **86**, 3851 (2001).

[10] V. M. Bedanov and F. M. Peeters, Phys. Rev. B **49**, 2667 (1994).

[11] M. Kong, B. Partoens, and F. M. Peeters, New J. Phys. **5**, 23.1 (2003).

[12] P. Ludwig, A. V. Filinov, M. Bonitz, and Yu. E. Lozovik, Contrib. Plasma Phys. **43**, 285 (2003).

[13] T. C. Killian, Nature (London) **429**, 815 (2004).

[14] T. Pohl, T. Pattard, and J. M. Rost, Phys. Rev. Lett. **92**, 155003 (2004).

[15] O. Arp, D. Block, A. Piel, and A. Melzer, Phys. Rev. Lett. **93**, 165004 (2004).

[16] J. P. Schiffer, Phys. Rev. Lett. **88**, 205003 (2002).

[17] R. W. Hasse and V. V. Avilov, Phys. Rev. A **44**, 4506 (1991).

[18] R. Rafac, J. P. Schiffer, J. S. Hangst, D. H. E. Dubin, and D. J. Wales, Proc. Natl. Acad. Sci. U.S.A. **88**, 483 (1991).

[19] K. Tsuruta and S. Ichimaru, Phys. Rev. A **48**, 1339 (1993).

[20] A complete table of ground state configurations for $1 \leq N \leq 160$ is available as accompanying material: P. Ludwig, S. Kosse, V. Golubnychiy, M. Bonitz, and H. Fehske, e-print physics/0409100.

[21] A. Filinov, M. Bonitz and Yu. E. Lozovik, J. Phys. A **36**, 5899 (2003).